Fabric and clay activity in soil water retention behaviour

Cristina Jommi[1,a] and Gabriele Della Vecchia[2]

[1]*Delft University of Technology, Department of Geoscience and Engineering, Stevinweg 1, 2628 CN Delft, The Netherlands*
[2]*Politecnico di Milano, Department of Civil and Environmental Engineering, piazza Leonardo da Vinci 32, 20133 Milano, Italy*

Abstract. Modelling the water retention behaviour requires proper understanding of all the processes which affect the amount of water stored in the pore network, depending on the soil state and the soil history. Traditionally, in many applications a single water content – suction curve is used. This approach limits the applicability of the retention data to practical cases, especially when fine grain soils are dealt with, when the deformability and activity of the clay fraction significantly affect the interaction with water. On the other side, water retention is being recognised more and more as a fundamental information in the description of the mechanical response of the soil, as it provides the key connection to the partial volumetric strains in a deformation process. With reference to the work performed at the Politecnico di Milano in the last years, a contribution on the understanding and modelling the coupled water retention- mechanical response in deformable soils is presented. The contribution aims to: (i) summarise the mechanisms which contribute to water retention; (ii) point out the role played by an evolving fabric and the fluid properties on water retention; and (iii) provide an overview on some of the consequences of evolving water retention properties on the mechanical behaviour.

1 Introduction

Water retention was early recognised as fundamental information to describe the hydraulic response of unsaturated soils [1]. Early studies pointed out the role of the type of clay and of clay content on the retention potential of soils. The role of organic content was also addressed extensively, as most of the models were developed for applications in the field of agronomy [e.g. 2,3]. Conversely, when unsaturated soil mechanics started being developed, most of the attention was devoted to compressibility and strength, in an attempt to describe the mechanical behaviour of unsaturated soils as a unique function of suction. The role of water retention on the mechanical response was initially disregarded, with the exception of the numerical analysis of unsaturated consolidation, which was requiring some information on water storage. Simple non linear functions, fitting available data on water content and suction were used to the scope [e.g. 4].

At the end of the '90s, inherent coupling between the retention mechanisms and the mechanical response started being investigated and included in models for unsaturated soil behaviour [e.g. 5-7]. A comprehensive approach to soil water retention was introduced by Romero and co-workers, who started analysing the role played by fabric on the retention properties of compacted soils [8,9]. Vaunat et al. [10] developed the first fully coupled hydro-mechanical model, which included an explicit description of the soil water retention behaviour.

In the last years, a huge body of research has been devoted to better quantify and model the influence of deformation on the water retention behaviour, especially focussing on the dependence of the air-entry value on the void ratio [11–14]. A more comprehensive insight into the role of the fabric on water storage can be provided by analysing the soil microstructure features by means of experimental techniques. In general, mercury intrusion porosimetry (MIP) is the preferred method to this aim, after Delage introduced its systematic use to analyse the consequences of mechanical loads on the pore size distribution (PSD) [15]. Mercury intrusion porosimetry has a number of limitations, which were recently reviewed by Romero and Simms [16]. Most importantly, MIP provides only a scalar measure of the apparent size of interconnected pores, while the pore network topology depends on the complex 3-D fabric of the different structure levels of the soil. Nonetheless, relevant basic information can be extracted from MIP data, which can be used to account for the soil fabric evolution in modelling the unsaturated soil behaviour.

Multiscale hydro-mechanical coupling is suggested by MIP data. This originates from the interplay behaviour of the different microstructure levels. At the scale of element testing in the laboratory, the hydraulic and the mechanical response depend on the mutual interaction between the different fabric levels, which govern the internal evolution of the soil microstructure. Some of these aspects are discussed hereafter, based on the work performed by the authors in the last years.

[a] Corresponding author: c.jommi@tudelft.nl

2 Water retention in soils

Traditionally, water retention in soils is claimed to be described by a "soil water retention curve", also called sometimes "soil water characteristic curve". Actually, different mechanisms contribute to the current amount of water stored into a given soil, which cannot be fully described by a single curve, nor is a characteristic of the soil. More properly, a water retention domain must be described, which reflects the dependence of the adsorption and storage potential of a soil from the current fabric and from its interaction with a specific fluid.

In the formulation of conceptual water retention models, stored and adsorbed water have been traditionally quantified in different ways in the various fields of application. Either mass based measures like water content, w (mass of water over solid mass), or volumetric measures, as volumetric water content θ_w (volume of water over total soil volume) and degree of saturation S_r (volume of water over volume of voids), have been adopted. Each of the previous measures presents advantages and shortcomings, as in an evolving fabric neither the mass, nor the volume can play the role of a constant reference [17]. The water ratio, e_w (volume of water over solid volume) might be somehow preferred, as it physically represents a measure of the mass of water (to which energy is referred), it can directly substitute the water ratio, $e_w = w\, G_s$, where G_s is the specific density of the soil particles, and it can be equally used as a measure of the degree of saturation, when normalised to the void ratio e, $S_r = e_w / e$.

Romero and Vaunat [9] used the water ratio in their fundamental paper, which was the starting point of many following developments. Their conceptual synthesis, copied in figure 1, clarifies the different exchange and retention mechanism, which dominates the storage response in the different suction ranges.

The multiscale character of water retention is also demonstrated in figure 1: in the lower suction range, a storage mechanism prevails, which depends on void ratio.

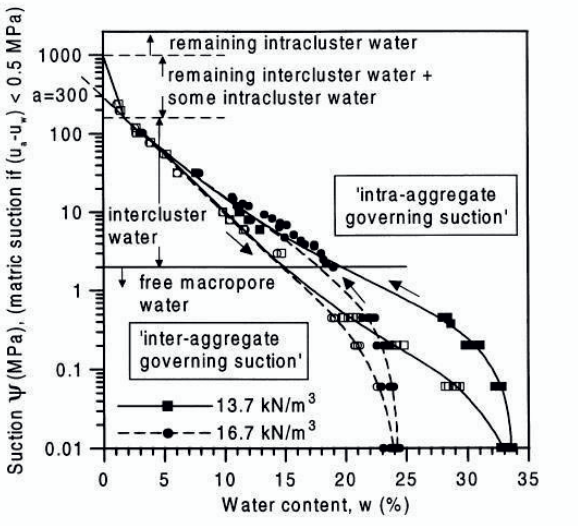

Figure 1. Water retention domain of Boom clay compacted dry of optimum, showing the different levels of fabric in which water can be stored (from Romero and Vaunat [9]).

At low water contents, the influence of initial and current void ratio is less significant, as the suction–water content relationship is mainly dependent on the mineralogical composition of the clay. Also, Romero et al. [8] and Romero and Vaunat [9] evidenced that a link exist between the different physical mechanisms dominating water storage in the different suction intervals and the pore size distribution, PSD, of the soil.

3 Evolution of water retention properties

Experimental evidence, especially on compacted soils, showed that the fabric of a given soil is not unique. It was demonstrated that the size of the aggregates is sensitive to the compaction water content [18], to the chemical composition of the pore fluid [19], and to the hydromechanical path history [20]. Furthermore, the fabric developed during the soil formation is not fixed, but evolves along multiphysics generalised stress path, as discussed in [21-24].

Sensitivity of the different classes of pores to hydraulic and mechanical paths was extensively discussed by Romero et al. [25], with reference to data on compacted Boom clay. In figure 2, the PSD of the as-compacted sample is compared to those of samples subjected to various hydromechanical paths after compaction. One sample was loaded at constant water content, a second one underwent wetting at constant volume, and the last one experienced free saturation at null vertical stress. The as-compacted sample is characterised by a bimodal distribution. Loading the sample at vertical stress of 0.6 MPa shifts the size of dominant macropores towards a slightly lower value, while the micropore volume and its dominant pore size are not affected.

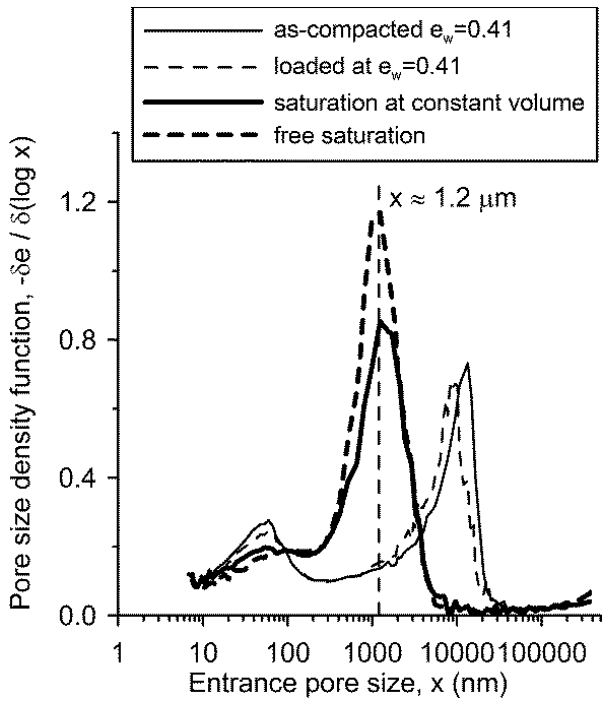

Figure 2. PSD functions of compacted Boom clay, subjected to different hydromechanical paths (from Romero et al. [25]).

On the contrary, the two saturation paths affect both inter-aggregate and intra-aggregate pores. After saturation, the two samples display a similar fabric dominated by a single peak, which is originated by both expansion of the micropores and reduction of macropores. The PSD function of a sample, which was further subjected to a drying path up to a total suction of 100 MPa after wetting at constant volume, showed that the inter-aggregate porosity eventually shrunk significantly, while the intra-aggregate porosity was almost completely recovered. The conclusion from the work was that the aggregate fabric tends to swell and shrink almost reversibly, becoming an inherent feature of the soil. On the contrary, the porosity between the aggregates suffers from irreversible modifications, and it is responsible of the irreversible strains observed at the laboratory test scale.

3.1 Modelling the water retention domain

The previous experimental observation promoted the development of a multiscale approach in modelling the water retention domain, which is based on the separation between intra-aggregate and inter-aggregate water ratios, having different evolution rules. The separation reads:

$$e_w = e_{wm} + e_{wM} \tag{1}$$

where the subscripts m indicate the intra-aggregate and M the inter-aggregate water ratios, respectively. The intra-aggregate pore volume was assumed to evolve reversibly. For water ratios lower than a characteristic value e^*_m, the aggregates are unsaturated, and the inter-aggregate voids are empty. Vice versa, for $e_w > e^*_m$, the aggregates are saturated, and the available water also partly fills the inter-aggregate voids. The delimiting value between the two regions, e^*_m, belongs to the $e_w = e_m$ line, and describes empty inter-aggregate voids and saturated intra-aggregate pore space. The data for $e_w > e^*_m$ are of interest in the description of the interaction between the two porosity levels. As a first approximation, a linear relationship between e_m and e_w was proposed to describe the evolution of the intra-aggregate pore volume:

$$e_m = e^*_m + \beta(e_w - e^*_m) \tag{2}$$

where the parameter β describes the slope of the approximating linear interpolation function and quantifies the swelling tendency of the aggregates.

Based on this assumption, a conceptual water retention model was presented by Romero et al. [25], and further discussed by Della Vecchia et al. [26]. Having assumed that the void ratio does not influence the intra-aggregate retention mechanisms, the intra-aggregate portion of the retention domain is delimited by fixed main wetting (W) and main drying (D) branches, uniquely linking the suction to a measure of water content:

$$e_{wD,W} = \frac{b_{D,W}}{\ln\left(\frac{s_{max}}{s^*_{mD,W}}\right)} e^*_m \left[\frac{b_{D,W} + \ln\left(\frac{s_{max}}{s^*_{mD,W}}\right)}{b_{D,W} + \ln\left(\frac{s}{s^*_{mD,W}}\right)} - 1\right] \tag{3}$$

where the subscripts D and W stand for the drying and the wetting branches, respectively. In the previous equation, e_w is the water ratio on the drying or the wetting branch of the curve, s_{max} is the value of suction corresponding to $e_w = 0$, $s^*_{mD;W}$ are the suction values corresponding to e_{wm}, that is, the smallest value of water ratio corresponding to saturated microvoids and empty macrovoids, on the drying and the wetting branches, respectively. The average slope of the two branches is given by the two parameters $b_{D,W}$.

The portion of the water retention domain that describes the retention mechanism of the inter-aggregate pore space may be scaled in the range $e \geq e_w \geq e_m$ with the expression:

$$\mathrm{e_{wD,W}} = \mathrm{e_m} + (\mathrm{e} - \mathrm{e_m})\left[1 - \frac{\ln\left(1 + \frac{\mathrm{s}}{\mathrm{s_{mD,W}}}\right)}{2}\right] \cdot \left[\frac{1}{1 + \left(\alpha_{\mathrm{D,W}}\mathrm{s}\right)^{\mathrm{n_{D,W}}}}\right]^{\mathrm{m_{D,W}}} \tag{4}$$

where the subscripts D and W again indicate the drying and the wetting branches, respectively.

The microscopic void ratio e_m was continuously adjusted following the relationship in Equation (2). In this way, swelling of the aggregates, and therefore, reduction of the inter-aggregate pore volume at constant void ratio by invasion of the aggregates, is explicitly taken into account by the parameter β. Explicit introduction of the intra-aggregate void ratio e_m and of its evolution in the phenomenological retention equations characterises the multiscale interaction at the hydraulic level. The variable s_m is assumed to change following the microscopic portion of the relevant branch of the water retention domain

$$s_{mD,W} = s^*_{mD,W} \exp\left[\frac{b_{D,W} e^*_m \left(b_{D,W} + \ln\left(\frac{s_{max}}{s^*_{mD,W}}\right)\right)}{e_{wmD,W} \ln\left(\frac{s_{max}}{s^*_{mD,W}}\right) + b_{D,W} e^*_m} - b_{D,W}\right] \tag{5}$$

Imposing the two analytical expressions in Equations (3) and (2) to be continuous together with their first derivatives in ($s_{D,W} = s_{mD,W}$, $e_w = e_{wm}$) gives a unique dependence of α on the set of independent parameters,

which implicitly describes the dependence of the air entry value, AEV, on the macroscopic void ratio.

In figure 3, experimental data of compacted Boom clay at different void ratios are compared with the model calibration. In spite of the model having been developed specifically on the experimental results from Boom clay, it proved able to reproduce the water retention domain for soils having different activity, as the comparison between data and calibrated curves for Barcelona silt and Febex bentonite, shown in figure 4, demonstrates.

It is worth noting that the model was formulated accounting for the experimental evidence from MIP data, which were partially exploited also on a quantitative basis to describe the microscopic void ratio evolution as a function of the water ratio. The number of parameters is comparable – or less – to that of other formulations developed to account for changes in the air entry value with void ratio. At the same time, as the formulation is physically based, some of these parameters can be inferred from basic soil properties, namely the Atterberg limits or the specific surface. The correlations presented in the papers by Romero et al. [25] and Della Vecchia et al. [27] provide the initial reference for the acceptable range of parameters. The model is able to track fabric changes, measured by the intra-aggregate and inter-aggregate porosities. Following Della Vecchia et al [27], the approach can be conceptually extended to any number of fabric levels.

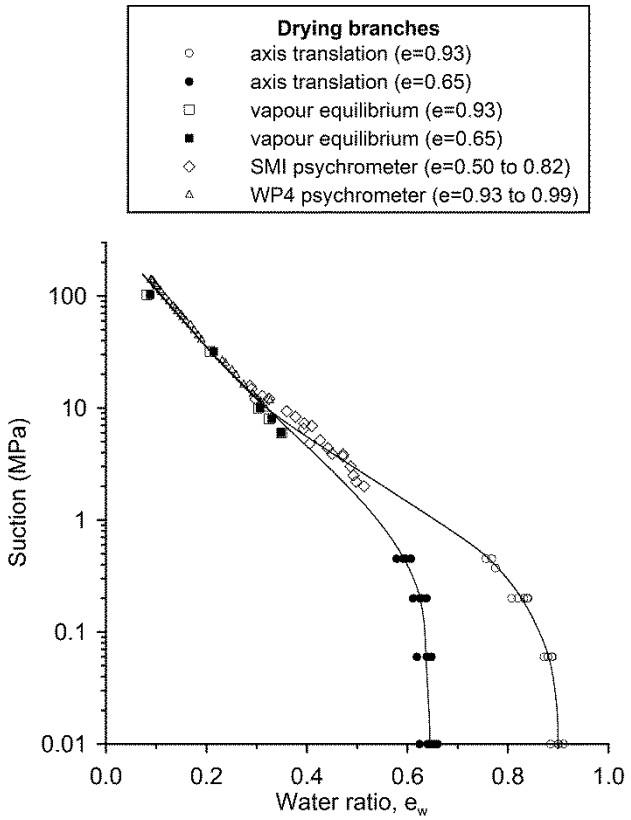

Figure 3. Water retention data and model for Boom clay compacted on the dry side of optimum (from Romero et al. [25]).

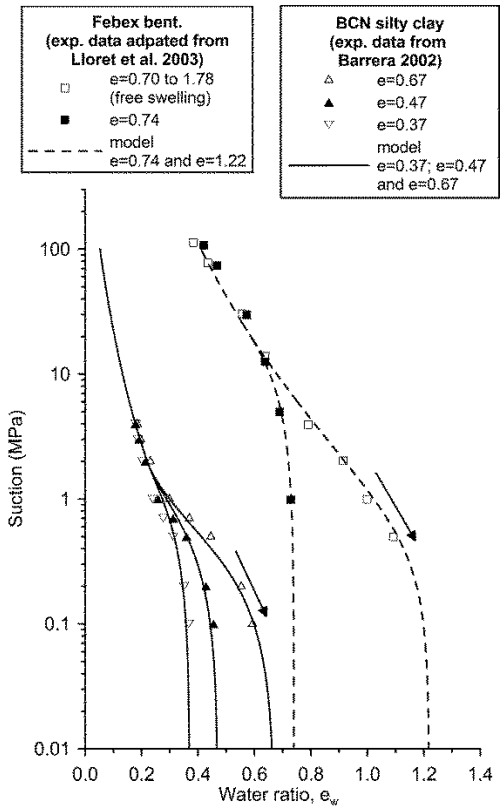

Figure 4. Water retention data and model for the wetting branches of the water retention domain of Barcelona silt and Febex bentonite (from Romero et al. [25]).

3.2 Influence of soil-water chemistry

The activity of the soil is dealt with by the parameter β, which actually is a function of the water chemistry too, for active soils. The influence of the water chemistry on the swelling potential of a given soil can be dealt with by changing β.

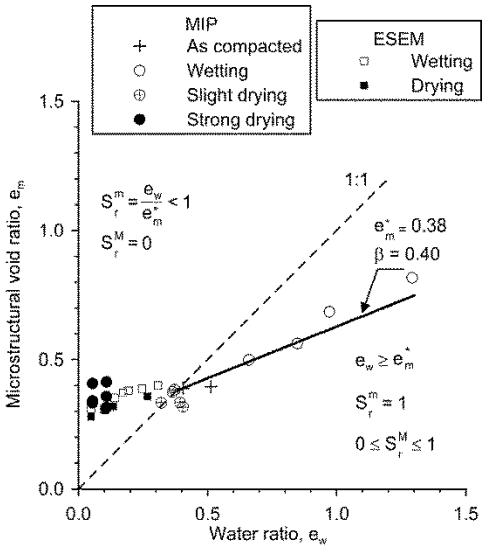

Figure 5. Evolution of microstructural void ratio with water ratio from MIP and ESEM data on compacted Boom clay (from Romero et al. [25]).

The role of β in the description of the microfabric evolution is demonstrated with reference to data on compacted Boom clay in figure 5. For water content in excess of e^*_m, the ratio between the microstructural void ratio, which measures the size of the aggregates, and the water content is measured by β. The linear approximation depicted in figure 5 can be used as a first approximation until saturated conditions are approached.

The parameter β quantifies how much the aggregates swell as a function of water availability. As swelling of the aggregates is due to the physico-chemical interaction of the solid particles with water, the chemical composition of water is playing a role too. Swelling of the aggregates will reduce the amount of macropores for a given total porosity, affecting the shape of the retention domain. An example is shown in figure 6, where the drying branches of the water retention curves of saturated bentonite-enriched sand mixtures, with active and inert bentonite, are compared. In the second case, the swelling potential of the bentonite was reduced by changing the chemical composition of the water by adding lead nitrate. The curves derived from MIP data clearly demonstrate the difference between the amount of water which can be stored in a swelling or non-swelling microstructure for a given suction. In figure 7 data from a wetting-drying path on the same material with active bentonite are simulated using a value of $\beta = 0.85$. Simulating inert bentonite by using a value of $\beta = 0.11$, would predict much lower values of water ratio for the same suction, as demonstrated by the continuous line in the figure.

Musso et al. [19] further exploited the approach in analysing the chemo-hydro-mechanical response of active clay, using MIP data to calibrate a relationship describing the dependence of the microscopic void ratio on the osmotic suction.

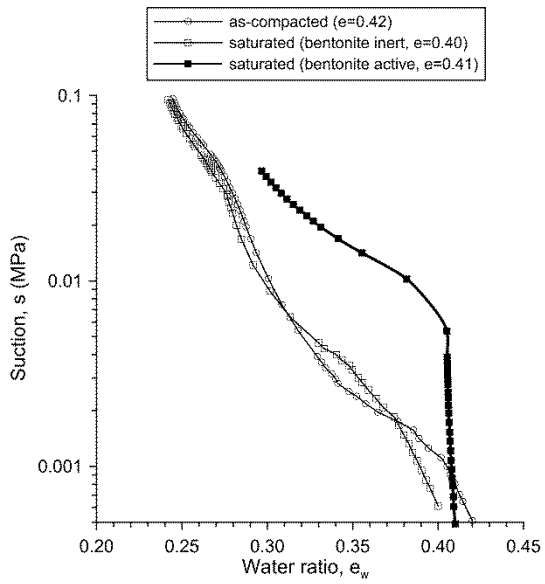

Figure 6. Drying branches of the water retention curves derived from MIP data for saturated bentonite-enriched sand mixtures, with active and inert bentonite, compared to the as-compacted state (from Romero et al. [25]).

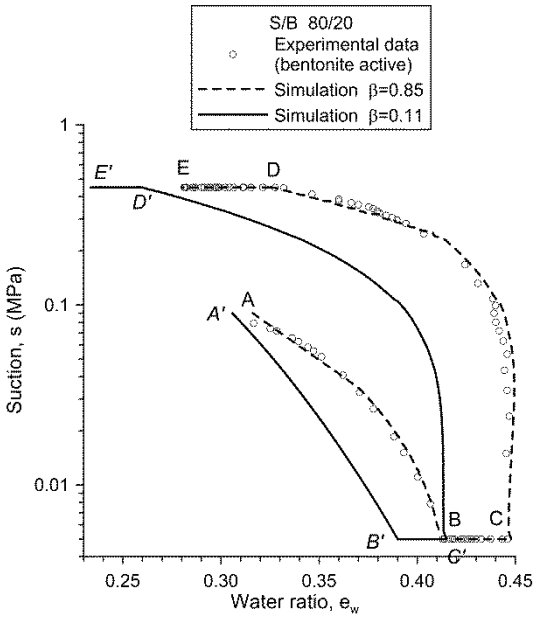

Figure 7. Water retention data for compacted bentonite-enriched sand with active bentonite compared to numerical simulations along the stress path ABCDE (from Romero et al. [25]).

4 Hydro-mechanical coupling

The evolution of the fabric, which governs the water retention potential, equally affects the mechanical response of soil. On the one hand, for a given water content, different suctions are expected for different soil fabrics. On the other hand, changing the size of the aggregates will change the amount and the size of the inter-aggregate pores, which are mostly responsible for the irreversible volumetric strains.

4.1 The role of volumetric strain on the retention domain

Experimental data on water retention typically show that the air-entry value, changes as a function of the void ratio. Advanced models for water retention [e.g. 11] tend to include this feature explicitly in the model equations. An interesting feature of the model recalled in the section 3.1 is that it implicitly predicts the evolution of the air-entry value, AEV, and of the air-occlusion value, AOV, with the total void ratio e and the intra-aggregate void ratio e_m, without adding any dedicated parameter. Model predictions of void ratio effects on the AEV and AOV of a compacted scaly clay are presented in Figure 8 (from [28]), compared with the values proposed in Airò Farulla et al. [29]. Model responses in terms of iso-suction lines is presented in Figure 9 in the plane (w;e), both for main wetting and main drying paths. The model correctly predicts the retention behaviour to be independent from the dry density for high values of suction: for $s > s_m$ the predicted iso-suction curves are vertical. For lower constant suction values, variation in void ratio implies variations in water content.

The difference between the main drying and the main wetting curves for a given suction defines the width of the hysteretic domain, which also changes with void

ratio. To characterise the hydraulic hysteretic behaviour of the material, Airò Farulla et al. [29] proposed a non-dimensional hysteresis index, HI, defined as

$$HI = 1 - \frac{A_w}{A_d} \tag{6}$$

where A_w and A_d are the areas subtended by the main wetting and the main drying curves, respectively, calculated as

$$A = \int_{s_{min}}^{s_{max}} e_w \, ds \tag{7}$$

The change in the hysteresis index as a function of void ratio predicted by the model is presented in Figure 10, together with the values calculated by [29]. The model is able to reproduce the increase of the size of the hysteresis loop with void ratio, again without introducing any dedicated parameter.

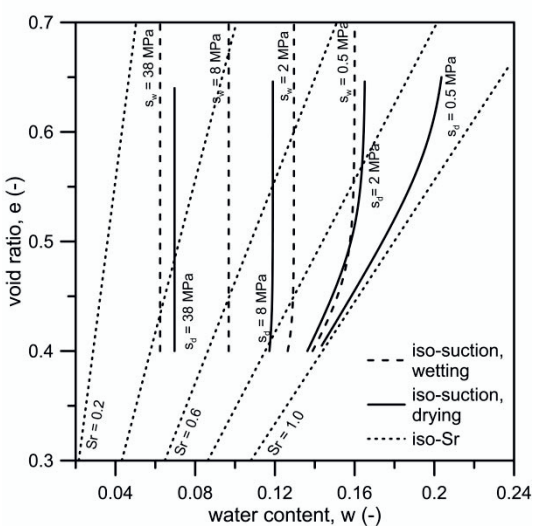

Figure 8. Water content vs. void ratio at constant suction. (from Della Vecchia et al. [28]).

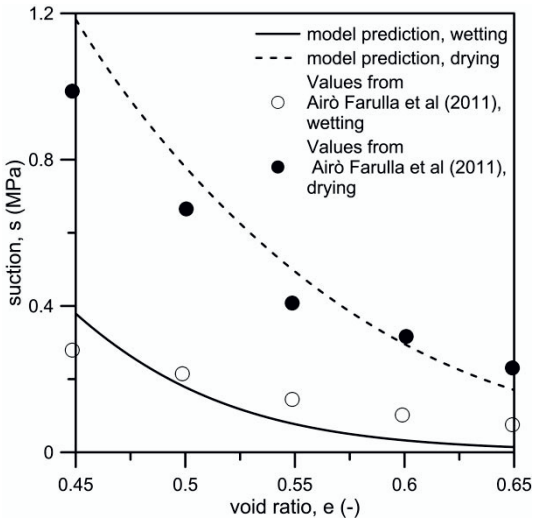

Figure 9. Evolution of AEV and AOV with void ratio: model predictions (from Della Vecchia et al. [28]) and data (from Airò Farulla et al. [29]).

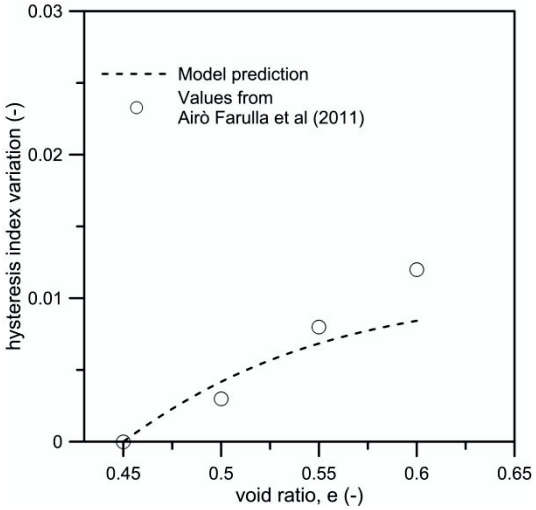

Figure 10. Model prediction of the hysteresis index variation (with respect to the reference void ratio e=0.45) with void ratio. (data from [29]).

4.2 The role of microfabric on the volumetric response

In the description of the mechanical response, different combination of "operative" stresses can be adopted for modelling the mechanical behaviour of unsaturated soils. Modelling the water retention as an integral part of the behaviour requires two stress variables to provide a complete formulation [30, 31]. Recently, Vaunat et al. [32] suggested a unified approach to stress variables, encompassing most of the previous choices, and linking the so-called Bishop's stress to the fabric evolution.

Here a simple volumetric average for the fluid pressures is used in the definition of the average skeleton stress:

$$\sigma'_{ij} = \sigma_{ij} - u_a \, \delta_{ij} + S_r \, (u_a - u_w) \, \delta_{ij} \tag{8}$$

where u_a is the air pressure, u_w is the water pressure and S_r is the degree of saturation (δ_{ij} is the Kronecker delta).

In the previous volumetric average, information on the water retention, depending on microstructural features, is essential in providing the link between the degree of saturation and the suction $s = u_a - u_w$. Besides, fabric evolution due to water content changes influences the stress–strain response of the material as well.

The experimental evidence suggests that the slope of the normal consolidation line is seldom constant with suction, even if expressed in terms of the average skeleton stress [33-36]. Koliji [36] suggested that this is a consequence of the influence of suction on the soil structure, where the term structure was used to indicate the combined effects of fabric, composition and interparticle forces. An increase in the post-yield compressibility in the effective stress plane at increasing suction was observed, which was interpreted as the experimental evidence of a plastic degradation mechanism. Because of suction, the preconsolidation pressure increases, and a state to the right of the virgin compression curve for saturated conditions may be

reached by the soil. Increasing the applied effective stress, the soil destructurates, and the compression index increases.

Similar evidence was recognised for compacted Boom clay [33]. Figure 11 shows the evolution of the elastic–plastic volumetric compliance in oedometer conditions $C_{oed} = -\Delta e/\Delta \ln \sigma'_v$ as a function of water ratio. The data were obtained from tests performed on samples prepared at different water contents, statically compacted at the same dry density (ρ_d = 1.37 Mg/m^3), and then subjected to compression in oedometer at constant water content. In the figure, other data from compaction stages at constant water content by Romero [37] are reported for comparison. The dependence of C_{oed} on water content was interpreted as a consequence of the related change of the size of the aggregates. To describe this dependence, a new state variable, D, was introduced by Della Vecchia et al [26,33], which describes the amount of available pore space invaded by the aggregates with respect to the current available pore space:

$$D = \frac{e_m - e_m^*}{e - e_m^*} = \beta \frac{e_w - e_m^*}{e - e_m^*} \quad (9)$$

The state variable D is a function of the parameters e_m and β, and it represents the mechanical counterpart of the influence of the size of the aggregates on the hydraulic behaviour. The variable D increases with the size of the aggregates, and it takes the value 0 for completely empty macrostructure and β in saturated conditions. While the dependence of the volumetric compliance on the water ratio is evidenced in Figure 11, Figure 12 clearly shows that the state parameter D, which represents a measure of the water ratio dependent fabric, is better able to normalise the elastic–plastic compliance data.

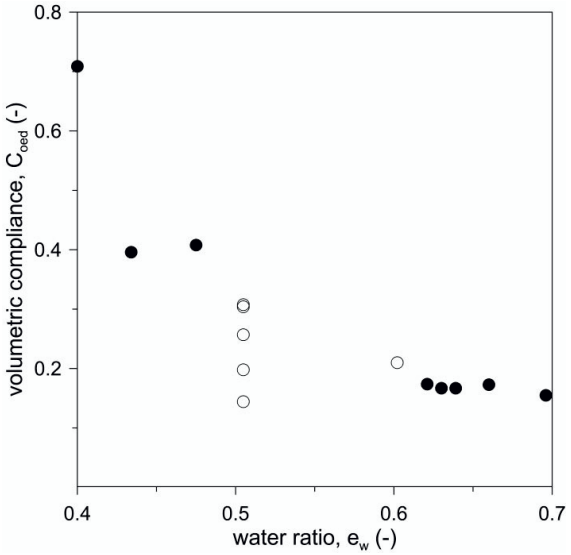

Figure 11. Evolution with water ratio of elastic-plastic logarithmic compliance under oedometer conditions for compacted Boom clay (data from [33] and [37]).

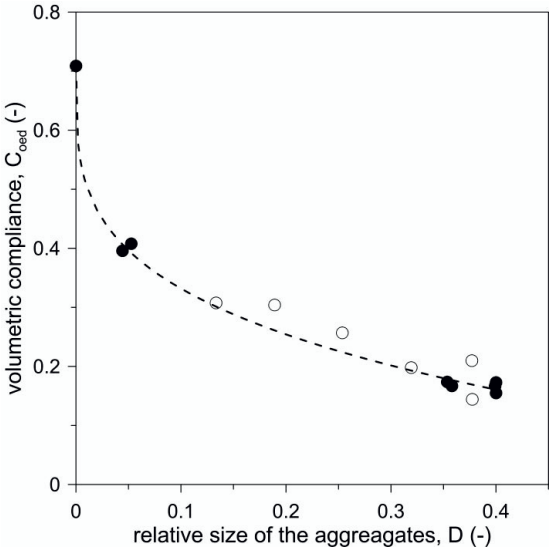

Figure 12. Evolution with the relative size of the aggregates of elastic-plastic logarithmic compliance under oedometer conditions for compacted Boom clay (data from [33] and [37]).

Further insight into the role of mutual interaction between the different fabric levels is provided by analysing the theoretical response of the inter-aggregate e_M and the intra-aggregate e_m voids during a cyclic isotropic wetting–drying test [26], shown in Figure 13. Intra-aggregate void ratio evolution was calculated by Equation (2), whereas e_M was obtained as the difference between the predicted values of total void ratio e and e_m. During the first wetting stage, e_m increases with increasing water content, despite the global collapse of the sample. During the subsequent drying–wetting cycle, a hysteretic response of the aggregate size is predicted. Reversibility of intra-aggregate evolution with water content implies a hysteretic response in terms of suction because of the nature of the adopted water retention model. Increase in e_m with decreasing e leads to a pronounced variation of the inter-aggregate void ratio e_M because of both global collapse of the sample and invasion of the aggregates in the inter-aggregate pores. In Figure 14, this concept is highlighted with reference to the first wetting stage. Reduction of the inter-aggregate void ratio Δe_M, defined as

$$\Delta e_M = \Delta e - \Delta e_m \quad (10)$$

can be interpreted as the sum of the contributions of the total collapse measured on the sample, $\Delta e_{coll} = \Delta e$, and of the invasion of the aggregates in the macrovoids $\Delta e_{inv} = -\Delta e_m$:

$$\Delta e_M = \Delta e_{coll} + \Delta e_{inv} \quad (11)$$

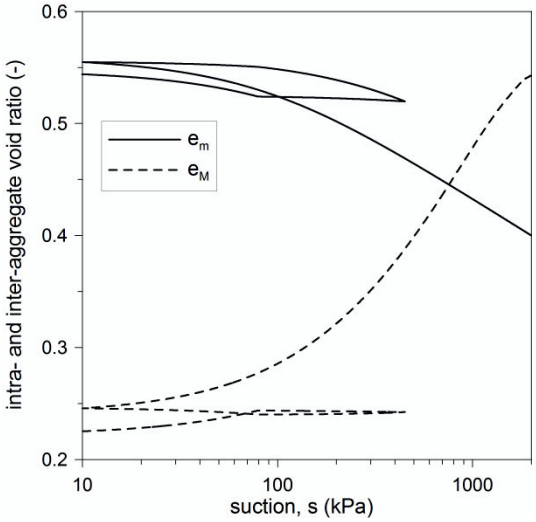

Figure 13. Predicted evolution of intra-aggregate and inter-aggregate void ratio with suction during an isotropic wetting test (from [26]).

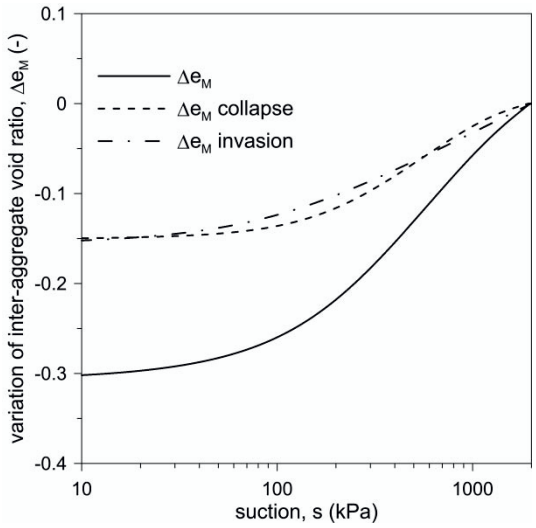

Figure 14. Variation of inter-aggregate void ratio during volumetric collapse (from [26]).

5 Selected applications in the context of earth constructions

The evolution of the fabric, which governs the water retention potential and the mechanical behaviour, is particularly relevant on the behaviour of compacted soils used in earth construction. Although the fabric created during compaction marks the response of the material, continuous interaction with the atmosphere and the groundwater produces irreversible strains, which change the hydro-mechanical response of the soil in the field, with respect to the as-compacted conditions. Two examples are briefly reported in the following. The first one refers to the Po river embankments, where samples retrieved from the field were used to quantify the change in the state of the compacted material during the lifetime of the construction. The second example shows the changes in the fabric estimated for a compacted soil stabilised with a biological technique.

5.1 Data from the Po river embankments

After a major flood occurred in 1952, which caused significant damage in the low Po river floodplain, an extensive investigation was started to characterise the typical soils, mainly clayey sandy silts, used in the construction of the flood protection embankments. One of the aims was to better quantify the optimal compaction conditions and verify the effectiveness in the field of the compaction procedures. Design specifications indicated that compaction should have guaranteed a dry density not lower than 95% optimum Proctor reference, with a tolerance on the water content of ± 2%. Data collected on samples retrieved in the field after compaction revealed that, in spite the design specifications being mostly respected, the actual as-compacted state was dominated by the seasonal variations in the water content of the available soil. During the wet season, higher water content resulted in compaction on the wet side of optimum with lower densities than the optimum. Conversely, in the dry season higher densities were usually obtained, but at the expenses of water content lower than the optimum.

Samples retrieved 250 days after the end of the construction, revealed that, irrespective of the initial as compacted state, the degree of saturation of the soil had increased and that the dry density had decreased, with more relevant changes for the samples compacted in the dry season [38].

Cyclic wetting-drying cycles, typically characterising the interaction of the earth construction with the atmosphere after the end of the construction, were simulated with the coupled hydro-mechanical model [39], to verify whether the fabric changes could be responsible of the evolution of the state of the samples in the field. The simulated as-compacted states are reported in Figure 15, together with the reference experimental compaction curves from [38]. In the figure, the simulated dry densities and water contents after cyclic wetting-drying are reported too. The results of the simulations fall in the same range of the samples collected in situ 250 days after the end of the construction, confirming that water content increases and dry density tends to decrease due to cyclic wetting-drying cycles experienced at the stress levels investigated.

A deeper insight into the coupled volumetric mechanisms may be provided by analysing the results of the numerical simulation of a wetting–drying–wetting cycle in detail. The results of the numerical simulations for the tests run imposing a net vertical stress of $\sigma_v = 10$ kPa are reported in Figures 16 and 17. An irreversible increment of water content is always to be expected as a result of the hysteretic retention mechanisms of compacted soils. Independently of the initial state of the compacted soil, the first wetting stage promotes an irreversible increase in water content. In the following drying and wetting paths the water content cycles in a smaller range. The results for void ratio, collected in Figure 17, highlight that if the soil is compacted at the wet of optimum it may undergo significant shrinkage upon first drying. The swelling strain depends slightly on the applied stress, but it is mostly governed again by the

retention properties of the soil. For the soil compacted wet of optimum, the main effect of suction is to act as an external load, hence inducing positive plastic volumetric strains.

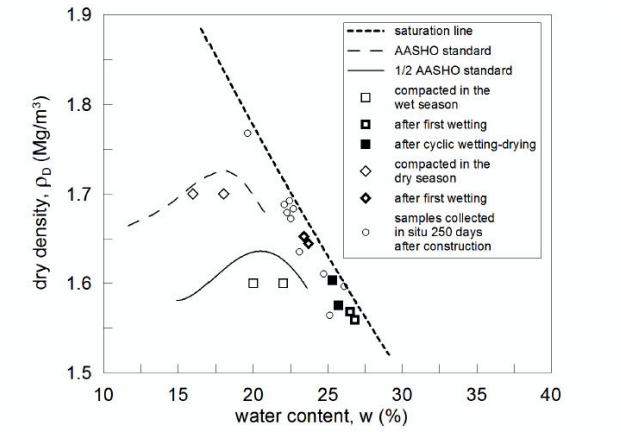

Figure 15. Simulated as-compacted states and states after a single and cyclic wetting stage (from Jommi & Della Vecchia [39]). Experimental data from [38].

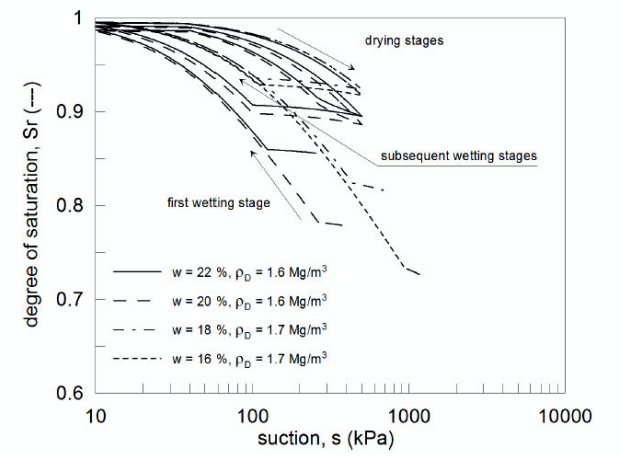

Figure 16. Simulated as-compacted states and states after a single and cyclic wetting stage (from Jommi & Della Vecchia [39]).

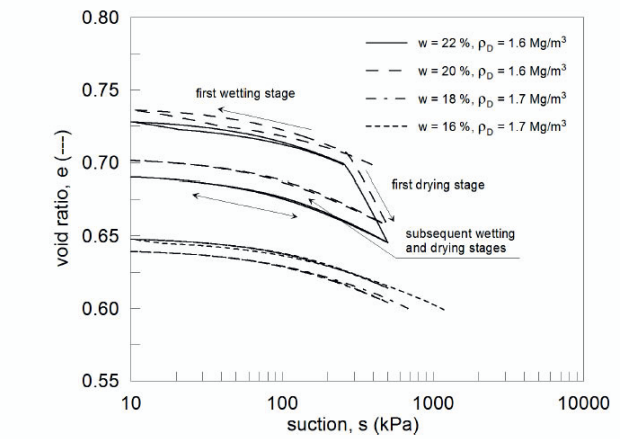

Figure 17. Simulated as-compacted states and states after a single and cyclic wetting stage (from Jommi & Della Vecchia [39]).

Following on the same line, Azizi [40] recently presented the results of a comprehensive investigation aimed at understanding the general consequences of drying-wetting cycles on the coupled hydromechanical response of compacted soils for earth constructions. The results of the study show that significant change in the fabric of the soil occur in the first drying-wetting cycles, which affect to a large extent the water retention properties, as well as the mechanical behaviour although to a less extent.

5.2 Biological improvement of compacted soils

A stabilisation technique, based on a microbiological treatment, was studied for different Iberian soils used in compacted linear earth constructions, resulting in the production of calcite by bio-mineralisation. To evaluate the advantages of the stabilisation procedure at the material level, laboratory tests were run on the soils, treated with different amounts of microorganisms during different treatment time intervals, and compacted afterwards [41]. The experimental data suggested that precipitation of calcium carbonate from bacteria had taken place in the pores which are slightly bigger than the characteristic size of the bacteria themselves. Comparison of hydro-mechanical data on the natural and the treated soils showed that the change in the pore size distribution is reflected consistently on the water retention properties, on the shear strength, and on the compressibility of the compacted samples. In view of the field applications, the data were exploited to develop a simple constitutive model for the stabilised soil, starting from the constitutive properties of its natural untreated counterpart [42].

Based on the results of the microstructure investigation [41], microbiological precipitation of calcite seems to produce two effects at the microscopic level. Firstly, it changes the pore size distribution due to microbiological calcite filling the pores having diameter in the range 3 μm ÷ 30 μm. Secondly, the liquid limit and the plasticity index of the soil decrease as the amount of microorganism increases.

The voids in which calcite precipitates do not seem to be affected by changes in the total void ratio, as the comparison between the relevant pore size distributions suggests (see [41]). Under this hypothesis, precipitation of calcite produces a decrease of the inter-aggregate pore space, with respect to the untreated sample, of an amount Δe^{BIO}:

$$e_M = e - (e_m + \Delta e^{BIO}) \tag{12}$$

in which the microbiologically affected pore volume may be estimated as:

$$\Delta e^{BIO} = \int_{3\mu m}^{30\mu m} (PSD_{nat} - PSD_{trated}) dD \tag{13}$$

Besides, as the plastic characteristics of the soil are slightly decreased by the presence of calcite, the value of e_m* decreased consistently (Fig. 18, from [42]).

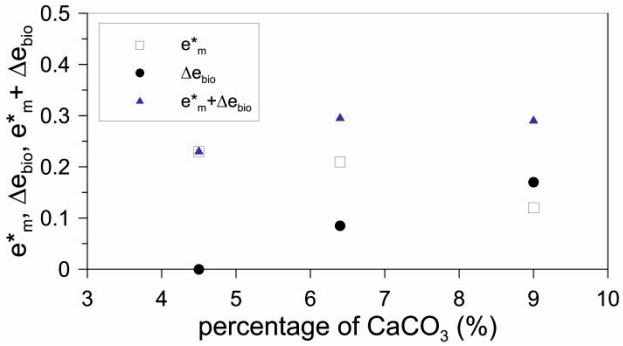

Figure 18. Variation of the microscopic pore space with calcite content at the end of the microbiological treatment (from [42]).

After compaction, specimens of different samples were loaded under vertical stresses representing the as-compacted condition in the field. They were further flooded at constant stress and eventually subjected to a loading-unloading cycle. The results showed that: (i) the amount of collapse induced by wetting was a function of the void ratio at the time of flooding, irrespective of the microbiological treatment; (ii) the biological treatment reduced the plastic compliance after collapse.

The hydro-mechanical oedometer tests were simulated by adopting the hydromechanical coupled framework presented in [43, 26]. The retention curves for the treated and the untreated soil were calibrated on the results of MIP data. The slope of the elastic-plastic compression line λ and the apparent pre-consolidation pressure were calibrated for the different samples on part of the data from the laboratory. All the other parameters were the same for the natural and the treated samples [42]. The comparison between the numerical simulations and the experimental data is reported in Figures 19 and 20. They show that a very good match can be obtained for both samples, adopting the same constitutive coupled hydro-mechanical approach, by suitable calibration of few parameters.

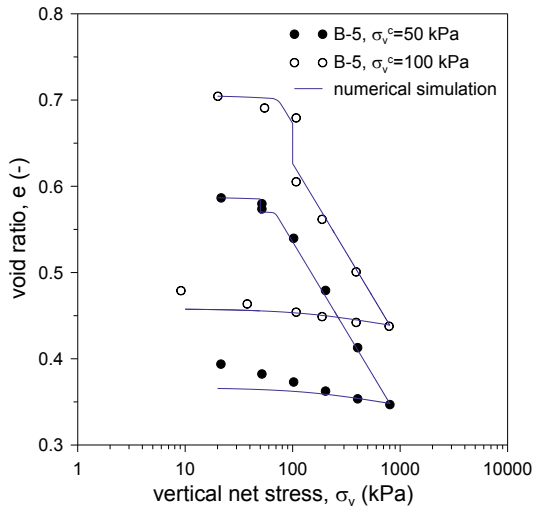

Figure 19. Comparison between experimental data (symbols) and numerical simulations of the oedometer tests on the original compacted soil (from [42]).

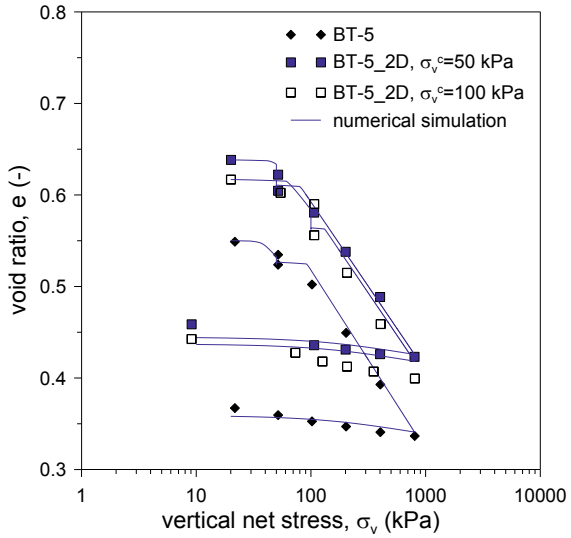

Figure 20. Comparison between experimental data (symbols) and numerical simulations of the oedometer tests on the compacted samples microbiologically (from [42]).

6 Conclusions

The results of the studies presented in this review summarise a number of findings, also coming from other research groups, which are considered to be relevant in the proper interpretation of the coupled hydromechanical behaviour of unsaturated soils. Although the work presented here mostly refers to compacted soils, the general principles equally apply to natural and reconstituted soils.

The key concept in the understanding of the water retention behaviour is that it is the macroscopic evidence of the mutual interaction of different fabric levels with water. This includes the chemical composition of water as far as it reacts with soil particles and aggregates.

The soil formation process gives the footprint of the hydraulic and mechanical response, but the following hydromechanical history affects the fabric of the soil, modifying its storage and deformational response. Water retention is not a characteristic of the soil neither it depends merely on void ratio. Although not complete, the pore size distribution is a better representation of the fabric features which influence the water storage, as well as the mechanical response. MIP can be usefully employed to this aim, as well as to detect relevant changes in the soil fabric during generalised hydromechanical paths.

An underlying assumption to this investigation, as well as all the other works cited, is that the different fabric levels are in thermodynamic equilibrium along any hydromechanical loading path. Removing this hypothesis will provide further insight into the time dependent behaviour of unsaturated soils, and a more general view on the dynamics of coupled process in unsaturated soils.

References

1. W.R. Gardner, Soil Science **85**, 228-232 (1958)
2. S.C. Gupta, W. Larson, Water Res. Res. **15**, 1633-1635 (1979)
3. T. Mayr, N.J. Jarvis, Geoderma **91**, 1-9 (1999)
4. A. Lloret, E.E. Alonso, Géotechnique **30** (4), 449-477 (1980)
5. S. Vanapalli, D. Fredlund, D. Pufhal, Géotechnique **49** (2), 143-159 (1999)
6. K. Kawai, S. Kato, D. Karube, *Proc. 1st Asian Conf. on Unsaturated Soils. Unsaturated Soils for Asia*, 329-334 (2000)
7. C. Ng, Y. Pang, J. Geotech. Geoenv. Eng. **126**(2), 157-166 (2000)
8. E. Romero, A. Gens, A. Lloret, *Eng. Geol.* **54** (1-2), 117-127 (1999)
9. E. Romero, J. Vanuat, *Experimental Evidence and Theoretical Approaches in Unsaturated Soils*, 91-106 (2000)
10. J. Vaunat, E. Romero, C. Jommi, *Experimental Evidence and Theoretical Approaches in Unsaturated Soils* 121-138 (2000)
11. D. Gallipoli, S.J. Wheeler, M. Karstunen, Géotechnique **53**(1), 105-112 (2003)
12. M. Nuth, L. Laloui, Comp. Geot. **35**, 835-844 (2008)
13. A. Tarantino, Géotechnique **59**(9), 751-762 (2008)
14. D. Masin, Int. J. Num. Anal. Meth. Geomech. **34**(1), 73-90 (2010)
15. P. Delage, G. Lefebvre, Can. Geot. J. **21**, 21-35 (1984)
16. E. Romero, P.H. Simms, Geotech. Geol. Eng. **26** (6), 705–722 (2008).
17. D. Masin, Engineering Geology **165**, 73-88 (2013)
18. R. Thom, R. Sivakumar, V. Sivakumar, E. Murray, P.A. MacKinnon, Géotechnique **57**(7), 469-474 (2007)
19. G. Musso, E. Romero, G. Della Vecchia, Géotechnique **63**(3), 206-220 (2013)
20. P. Delage, Géotechnique **60**(5), 353-368 (2010).
21. O. Cuisinier, L. Laloui, Int. J. Num. Anal. Meth. Geomech. **28**(6), 483-499 (2004).
22. A. Koliji, L. Laloui. O. Cuisinier. L. Vulliet, Transp. Porous Media **64**, 261-278 (2006).
23. R. Monroy, L. Zdravkoviv, A. Ridley, Géotechnique **60**(2), 105-119 (2010)
24. Q. Wang, A.M. Tang, Y.J. Cui, P. Delage, B. Gatmiri, Eng. Geol. **124** (4): 59-66 (2012).
25. E. Romero, G. Della Vecchia, C. Jommi, Géotechnique 61(4), 313-328 (2011).
26. G. Della Vecchia, C. Jommi, E. Romero, Int. J. Num. Anal. Meth. Geomech. **37**, 503-535 (2013).
27. G. Della Vecchia, A.C. Dieudonnè, C. Jommi, R. Charlier, Int. J. Num. Anal. Meth. Geomech. **39** (7), 702-723(2015).
28. G. Della Vecchia, C. Airò Farulla, C. Jommi, *Unsaturated Soils: Research and Application, Proceedings of the Second European Conference on Unsaturated Soils* 2, 55-62 (2012)
29. C. Airò Farulla, A. Battiato, A. Ferrari*, Unsaturated Soils. Proceedings of the Fifth International Conference on Unsaturated Soils* 1, 417–422 (2011)
30. A. Gens, *Proc. 1st Int. Conf. Unsat. Soils* (3), 1179-1200 (1996)
31. G.T. Houlsby, Géotechnique **47** (1), 193-196 (1997)
32. J. Vaunat, F. Casini, E. Romero, *submitted to Géotechnique* (2016).
33. G. Della Vecchia, PhD Thesis, Politecnico di Milano (2009)
34. S. Wheeler, V. Sivakumar, Gèotechnique **45**, 35-53 (1995)
35. D. Sun, H. Matsuoka, Y. Xu, Geot. Test. J. **27**(4), 362-370 (2004)
36. A. Koliji, PhD Thesis, EPFL (2008)
37. E. Romero, PhD Thesis, UPC (1999)
38. F. Colleselli, G. Cortellazzo, C. Jommi, R. Lagioia, *XX Italian National Congress of Geotechnics*, 435-443 (1999)
39. C. Jommi, G. Della Vecchia, *Mechanics of Unsaturated Geomaterials*, 353-373 (2010).
40. A. Azizi, PhD Thesis, Politecnico di Milano (2016)
41. L. Morales, E. Romero, C. Jommi, E. Garzón, A. Giménez, Acta Geotechnica (10), 157-171 (2015)
42. G. Della Vecchia, L. Morales, E. Garzon, C. Jommi, E. Romero, *Unsaturated Soils, proceedings of the Fifth International Conference on Unsaturated Soils*, 795-801 (2010)
43. E. Romero, C. Jommi, Water Resources Research **44**, W12412:1–W12412:16 (2008)